An apertureless near-field microscope for fluorescence imaging

T. J. Yang, Guillaume A. Lessard, and Stephen R. Quake[a]
Department of Applied Physics, California Institute of Technology, Pasadena, California 91125

(Received 18 August 1999; accepted for publication 16 November 1999)

We describe an apertureless near field microscope for imaging fluorescent samples. Optical contrast is generated by exploiting fluorescent quenching near a metallized atomic force microscope tip. This microscope has been used to image fluorescent latex beads with subdiffraction limit resolution. The use of fluorescence allows us to prove that the contrast mechanism is indeed spectroscopic in origin.
 [S0003-6951(00)00403-4]

The resolving ability of optical microscopy with far field optics is limited by the diffraction of light. Near field scanning optical microscopy allows one to take optical images with resolution below the diffraction limit.[1,2] In the traditional technique, light propagating through a waveguide is forced through a subwavelength aperture, which is then scanned in close proximity to a sample. Technical limitations relating to the skin depth of the metal used to coat the waveguide and various tip scanning artifacts result in a practical resolution of 30–50 nm.[3,4] To surpass this limit, apertureless near field scanning microscopes (ANSOM) were proposed and demonstrated, with apparent resolutions as low as 1 nm.[5–8] ANSOM techniques involve the use of an oscillating sharp probe, which is scanned over the sample. The probe perturbs an incident laser beam, either by introducing phase shifts in the electric field or by periodic occlusion of the sample. ac detection techniques are used to discriminate light scattered by near field interactions from the far field contribution. However, for these single wavelength microscopes the contrast mechanism is still not completely understood and on occasion the images are contaminated by topographical artifacts.[9] Recently a fluorescence ANSOM microscope (FANSOM) was demonstrated which uses the principle of a two photon excitation and electric field enhancement near the tip.[10]

Here we report the results of a new FANSOM microscope designed to image fluorescent samples with single photon excitation. We exploit the fact that fluorescent molecules transfer energy nonradiatively to proximate metal or semiconductor surfaces. This quenching effect has been studied for many years[11] and may limit the effectiveness of microscopes using electric field enhancement as a contrast mechanism.[10,12] The ability to use single photon excitation allows greater flexibility in the choice of laser source and reduces the peak power through the objective and on the sample. The use of fluorescence facilitates interpretation of the images and provides compelling evidence that the contrast mechanism is indeed optical in origin. Specific spectroscopic effects such as photobleaching are observed, showing that there is no height contamination in the optical image. As with ANSOM, the resolution is determined by the radius of curvature of the probe. AFM tips with 5 nm radius of curvature are now commercially available, and carbon nanotube AFM tips have been demonstrated.[13] It is thus reasonable to expect that the ultimate resolution of FANSOM will be in the 1–5 nm range. There are a number of important possible applications of FANSOM, including imaging of single DNA molecules for optical mapping and fluorescent *in situ* hybridization,[14] spectroscopy of nanoparticles[15] and quantum well devices,[16] and the possible extension to single molecule Raman imaging.[17]

We used our FANSOM to image fluorescent latex particles with subdiffraction limit resolution and to measure fluorescence photobleaching, proving that the contrast mechanism is due to a near-field effect and is optical in nature. The experimental setup is shown in Fig. 1. It consists of a tapping mode atomic force microscope (AFM) on top of an inverted optical microscope, both homemade. The sample is scanned under the tapping AFM tip (resonant frequency ~250 kHz), while a green HeNe (543.5 nm, Uniphase 1674P) laser beam is focused to a diffraction limited spot on

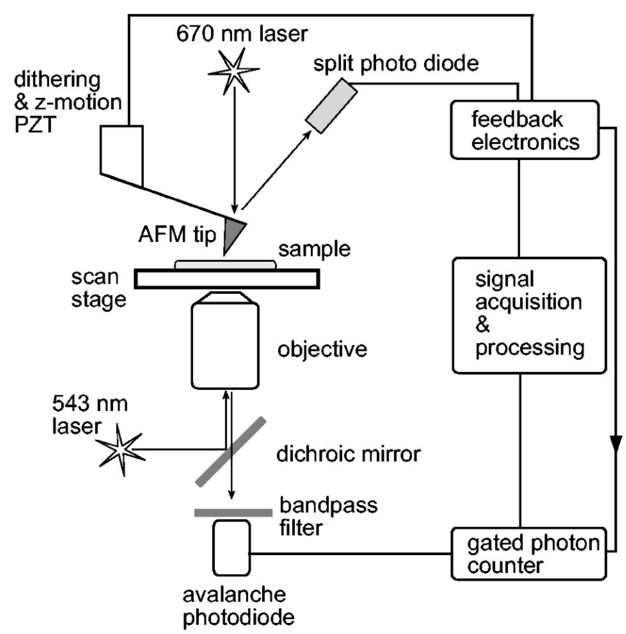

FIG. 1. A schematic diagram of the apparatus. A tapping mode AFM was built on top of an inverted microscope. A laser beam from a green HeNe was focused on the AFM tip, while the sample was scanned in the *xy* plane. Fluorescent photons were detected by an avalanche photodiode and processed by a gated photon counter that was triggered by the measured height of the AFM cantilever. The pixel acquisition time was 40 ms, allowing approximately 8000 taps of the AFM tip per pixel.

[a]Electronic mail: quake@caltech.edu

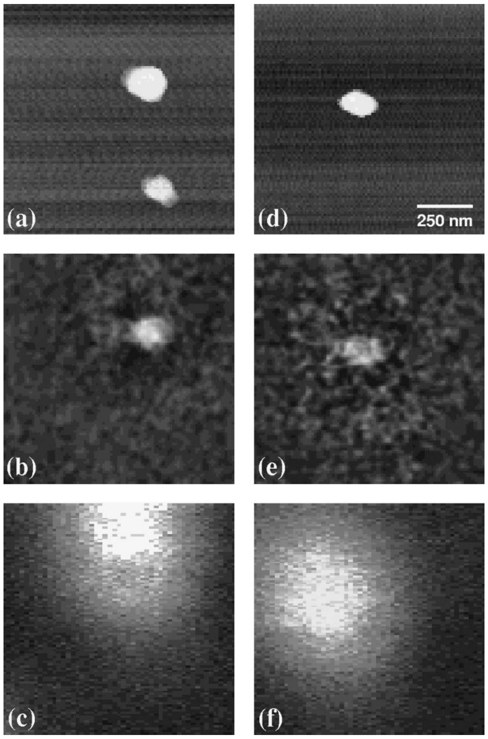

FIG. 2. Two sets of images of 60 nm latex beads; (a) and (d) are AFM images; (b) and (e) are FANSOM images; and (c) and (f) are images of the far field fluorescence. The FANSOM images have been low pass filtered by convolving with a Gaussian of radius 1 pixel. In image (a), the AFM detected a nonfluorescing contaminant particle that is not visible in the corresponding FANSOM (b) or far field optical (c) images, providing further evidence that the contrast mechanism is optical.

the tip via a microscope objective. Commercial silicon AFM tips (nanosensors) were coated with a 60 nm layer of gold by thermal vacuum deposition. Photons emitted by fluorescence are collected by the same objective (Olympus Plan Apo Chromat 60×, 1.4 NA) and imaged onto a photon counting avalanche photodiode (EG&G SPCM 100), whose output is in turn processed by a gated photon counter (Stanford Research Systems SR400) to implement a lock-in detection scheme. The gating was triggered by the position of the AFM cantilever such that the counts measured while the tip was closest to the sample were subtracted from the counts measured when the tip was farthest from the sample. This effectively selects a 100 Hz frequency window centered on the 250 kHz resonant frequency of the cantilever and allows discrimination of the far-field emission from the photon suppression due to fluorescence quenching at the near field of the tip. The position of the AFM cantilever was measured on a split photodiode using a standard optical lever scheme. The split photodiode signal was used as part of a feedback loop to maintain constant tapping amplitude, and was also used with a phase locked loop to trigger the photon counter gates.

During image acquisition, the sample was scanned in the *xy* plane and two signals were collected: the photon counter difference output (optical) signal and the AFM *z*-feedback (topographical) signal. This allows the simultaneous acquisition of topographical (AFM), and near field optical fluorescence (FANSOM) images. Far-field optical images using the total number of photons per pixel were also taken during a separate scan. Our samples consisted of 60 nm fluorescent latex beads (Nile Red, Interfacial Dynamics Corp.) deposited on an RCA cleaned glass cover slip. The laser beam had a total power of 20 nW focused into a 500 nm diameter spot. We used a set of bandpass filters in front of the avalanche photodiode that selected out the region between 580 and 620 nm, excluding both the 543.5 nm excitation light and the 670 nm diode laser used for the AFM feedback.

Figure 2 shows two sets of images collected from a 1 μm^2 field of view. Fluorescent beads are seen using AFM, FANSOM, and far field imaging. In one image [Fig. 2(a)], there is also a nonfluorescing contaminant particle that is visible in the AFM image but not in the corresponding FANSOM [Fig. 2(b)] or far field [Fig. 2(c)] images. We estimated the resolution of the FANSOM microscope by tak-

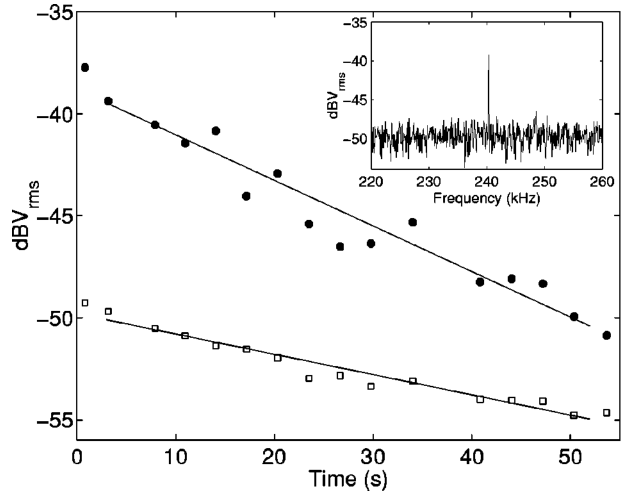

FIG. 3. The AFM tip was positioned over a 100 nm fluorescent bead and measured the power spectrum of the avalanche photodiode. There is a clear peak at the resonant frequency of the AFM cantilever (inset) that is only present when the bead is fluorescing. We increased the incident power to 60 nW and plotted the height of that peak as a function of time as the bead photobleached, and saw a corresponding reduction in the peak height until it disappeared into the noise. The background level of the power spectrum also decayed, but more slowly.

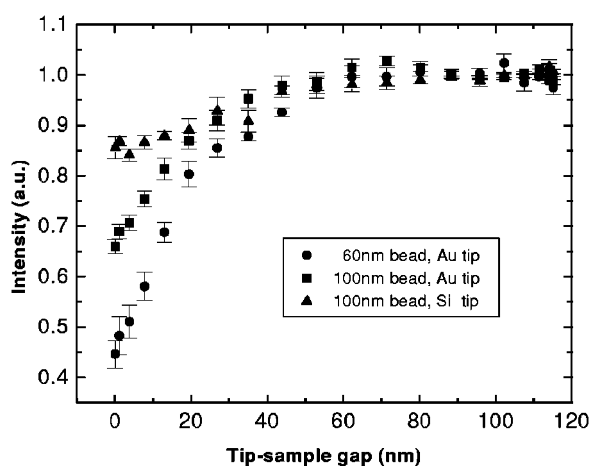

FIG. 4. The approach curves show that as the tip approaches the sample, the fluorescence decreases. The effect is more significant for gold coated tips than for bare silicon ones. The approach curve was obtained by scanning the gate of photon counter through the entire tapping period. The gate width was 1/40 of period, and 30 000 gates were opened at a given tip position to make each data point. The photon counts were normalized to show the quenching efficiency. Only one half of the period is displayed for simplicity. Each curve in this figure is an average of five curves for gold coated tips, and two curves for silicon tips.

ing a vertical line slice through the center of the beads and measuring the full width at half maximum of the peak, finding 95 and 120 nm. Given that the bead has a 60 nm diameter, we can estimate the resolution of the FANSOM to be between roughly 30 nm, well below the diffraction limit of 260 nm. Although this method of determining the resolution does not strictly adhere to the classical Rayleigh criterion, it does show unambiguously that the resolution surpasses the diffraction limit. Control images taken with the tip removed show only the expected far-field image, with no signal in the FANSOM image. Control images taken with the green laser blocked show no FANSOM image, only the normal AFM image.

We verified that the FANSOM image is not contaminated with height information by observing photobleaching of the bead. Repeated images of the same bead showed a gradual reduction in the level of the FANSOM signal, while the AFM image remained unchanged. We also took images with 100 nm beads excited by a 60 nW laser beam. By positioning the AFM tip directly above a single bead, we were able to observe the near-field signal as a function of time. We measured the signal in this case as the height of a peak in the power spectrum of the output of the avalanche photodiode (Fig. 3). The resonance is present only when the tip and the laser are aligned, and only when the incident laser is present. The signal gradually decreases with time as a result of photobleaching. At the end of the measurement we verified that there had been no significant drift of the AFM tip position. In previous work, we have observed a similar effect with bare silicon tips and shown that it is due to near field effects.[18]

To prove that the contrast mechanism is due to fluorescent quenching, we measured the signal intensity as a function of tip-sample separation (Fig. 4). These approach curves show that the fluorescence decreases dramatically as the tip approaches the sample, and that the quenching effect occurs over an ~ 10 nm distance (± 2 nm), i.e., in the near field of the tip. The overall contrast when imaging is determined by the modulation depth of the signal, i.e., the amount of quenching relative to the far-field signal. The approach curves show that the modulation depth of the signal is greater than 50% for 60 nm beads when gold coated tips were used, and increases as the size of the feature is reduced.

In conclusion, we have demonstrated subdiffraction limit near field fluorescence imaging with an apertureless probe. We have verified the near field effect and demonstrated that the images are free from topographical artifacts. In future work, we plan to test the ultimate sensitivity of the FANSOM by imaging single dye molecules and biological samples.

The authors thank Pierre Barritault and Francisco Guzman for contributions in the early stages of this work and Jeff Kimble for the generous loan of equipment. This work was supported in part by the Keck Foundation. G.L. had partial financial support from the Fonds FCAR.

[1] D. W. Pohl, W. Denk, and M. Lanz, Appl. Phys. Lett. **44**, 651 (1984).
[2] A. Harootunian, E. Betzig, A. Murray, A. Lewis, and M. Isaacson, J. Opt. Soc. Am. A **1**, 1293 (1984).
[3] B. Hecht, H. Bielefeldt, Y. Inouye, D. W. Pohl, and L. Novotny, J. Appl. Phys. **81**, 2492 (1997).
[4] V. Sandoghdar, S. Wegscheider, G. Krausch, and J. Mlynek, J. Appl. Phys. **81**, 2499 (1997).
[5] F. Zenhausern, M. P. O'Boyle, and H. K. Wickramasinghe, Appl. Phys. Lett. **65**, 1623 (1994)
[6] Y. Inouye and S. Kawata, Opt. Lett. **19**, 159 (1994).
[7] R. Bachelot, P. Gleyzes, and A. C. Boccara, Microsc. Microanal. Microstruct. **5**, 389 (1995).
[8] B. Knoll and F. Keilman, Nature (London) **399**, 134 (1999).
[9] Y. Martin, F. Zenhausern, and H. K. Wickramasinghe, Appl. Phys. Lett. **68**, 2475 (1996).
[10] E. J. Sanchez, L. Novotny, and X. S. Xie, Phys. Rev. Lett. **82**, 4014 (1999).
[11] R. R. Chance, A. Prock, and R. Silbey, in *Advances in Chemical Physics*, edited by I. Prigogine and S. A. Rice (Wiley, New York, 1978), Vol. 37, p. 1.
[12] Y. Kawata, C. Xu, and W. Denk, J. Appl. Phys. **85**, 1294 (1999).
[13] H. J. Dai, J. H. Hafner, A. G. Rinzler, D. T. Colbert, and R. E. Smalley, Nature (London) **384**, 147 (1996).
[14] X. Michalet, R. Ekong, F. Fougerousse, S. Rousseaux, C. Schurra, N. Hornigold, M van Slegtenhorst, J. Wolfe, S. Povey, J. S. Beckmann, A. Bensimon, Science **277**, 1518 (1997).
[15] S. A. Empedocles, D. J. Norris, and M. G. Bawendi, Phys. Rev. Lett. **77**, 3873 (1996).
[16] H. F. Hess, E. Betzig, T. D. Harris, L. N. Pfeiffer, and K. W. West, Science **264**, 1740 (1994).
[17] S. Nie and S. R. Emory, Science **275**, 1102 (1997).
[18] G. A. Lessard, T. J. Yang, P. Barritault, and S. R. Quake, Proc. SPIE **3607**, 158 (1999).